

ON THE EFFECTS OF THE INTERPHASE ON THE DAMPING OF CFRP STRUCTURES: AN EXPERIMENTAL INVESTIGATION

Mattia Gasenge¹ , Paolo Sebastiano Valvo¹ , Laura Aliotta¹ , Andrea Lazzeri¹ 

¹ University of Pisa, Department of Civil and Industrial Engineering, Largo Lucio Lazzarino, IT-56122, Pisa, PI, Italy

✉ corresponding author: m.gasenge@studenti.unipi.it

Received: 2023-11-30 / Accepted: 2024-04-09 / Published: 2024-06-18

ABSTRACT

The increased adoption of composite laminates in modern engineering requires advancement in the prediction of their dynamic behavior. Damping is a major design constraint in aerospace structures subjected to cyclic loads. While the effects caused by damping are well known, the mechanisms that cause it at the microscopic level are still unclear on a quantitative basis. Testing of these phenomena requires some difficulties to be overcome, like the contribution of spurious sources. The study focuses on the effects that the interphase has on the damping properties of carbon fiber-reinforced polymer (CFRP) composite structures. Three-phase models are employed to investigate the dependence of damping on the interphase mechanical properties, with a focus on the fiber-matrix interfacial shear strength. The experimental campaign confirms the attended results: in particular, a stronger interphase determines a lower damping of the structure.

KEYWORDS: damping, interphase, CFRP, free decay, silanes

1. Introduction

The contribution of the interphase to the damping of a composite structure is not newly discovered, as extensive research was conducted at the time when composite materials started their rapid diffusion in the aerospace industry. Some of the most relevant concepts discovered and validated since then are summarized in the recent review by Tang and Yan [1]. Damping in composite structures is dominated by the matrix viscoelastic behavior. When the bond between fibers and matrix is weak though, the interphase contribution to damping is relevant and may play a fundamental role because it allows to sensibly affect damping, while leaving the other mechanical properties nearly unchanged [2]. Two main mechanisms are happening at the interface level that contribute to damping: the damping due to the viscoelastic nature of the interphase, and the friction between the two surfaces of a crack when the structural health of the interphase is no longer guaranteed. The elastic limit of the interphase is the discrimination point between the two mechanisms. It is a widely agreed fact that the damping of a structure increases in materials with weaker interphases. This result has been validated by different investigators [3-5]. It is also an acknowledged fact that damping is higher for shear stresses. Indeed, this is one of the reasons why the interphase is so important in damping, being a point of concentration for shear stresses. For these reasons, three-phase models that take the interphase into account have been developed. The Chaturvedi and Tzeng model [6] is based on the Coxian two-phase representative volume element

(RVE) model, modified to include a third phase. The model can be employed with an energy model or with a force balance to calculate the loss factor.

Murayama and Lawton in 1973 [7] published one of the few studies where the inverse relationship between damping and interface strength is quantified, not just shown as a qualitative statement. From the three-point plot of damping versus interface strength, a linear path is individuated, suggesting a direct proportionality between the interface strength and the damping with a negative coefficient of proportionality.

The interphase can be modified in multiple ways [8] by suitably treating the fiber surface. In this way, specimens can be obtained where the fibers and matrix are the same, and only the interphase changes. The most common methods for fiber surface treatment include: oxidation (acidic [9] or electrochemical [10]), which is effective and relatively cheap, but affects the mechanical properties of the fiber due to etching; nano-sized particles coating [11,18]; plasma treatment [12], a very precise and versatile technique, used on laboratory scale, but which is not so effective due to the low number of oxygen functional groups that can be generated on the fiber's surface; silane coupling agents grafting [13,19], which provides an abundance of functional groups and establishes a strong chemical bond between the fiber and matrix. But the inertness of carbon fibers hinders the grafting potential of the silanes.

In an attempt to exploit the advantages, while damping their downsides, these technologies have also been mixed together [14,15]. The strategy followed by these two investigators, and replicated in the present work, is to pre-treat the surface to generate active oxygen groups on the surface of the fibers, so that the successive grafting of silane coupling agents can benefit of a superior compatibility with the fiber.

Silanes have the peculiar property of presenting a hydrophilic part, that can react with the fiber surface, and a hydrophobic part on the other end that can react with the matrix. Therefore, they act as a bridge that allows for the selective enhancement of damping without causing substantial alterations to the bulk mechanical properties of the composite material.

Oxidation of the fiber surface has been achieved by using hot air in an oven as a gaseous medium. This treatment [16] causes the formation of numerous hydroxyl and carboxyl groups on the fiber surface that can react with the epoxy group. In addition, the oxidation of the surface increases its roughness, therefore improving the mechanical interlocking mechanism.

The present work aims at quantifying the effects of the interface mechanisms on damping through an experimental campaign on a set of specimens with different interphases.

2. Analytical discussion

The Chaturvedi and Tzeng model can be used to try to derive an analytical expression that describes Murayama's plot. From Ungar and Kerwin 1962 [17], the loss factor of a composite can be calculated as a weighted mean of the loss factors of each constituent phase weighted on the strain energy stored in each phase. Chaturvedi and Tzeng provide the analytical expressions for each one of the strain energies, but for the following discussion only the interphase strain energy must be considered. If the shear stress is taken to be equal to the interfacial shear strength (IFSS) value, then the strain energy expression simplifies as follows:

$$W_i = \frac{V_i}{2G_i} IFSS^2 \quad (1)$$

where W is the strain energy, V is the volume fraction, G is the shear modulus, and the subscript i refers to the interphase. The differences in the loss factor of a surface treated composite against the loss factor for an untreated composite must be computed. The total strain energy in the composite

can be assumed to be equal, given the negligible impact that the interphase has on stored energy, as demonstrated by Kennedy et al. [2]. So, the only quantities that differ between the two materials are the strain energy and damping of the interphase. The resulting differential loss factor becomes

$$\Delta\eta = \frac{1}{2W_c} \left(\frac{V_{i,u}\eta_{i,u}}{G_{i,u}} IFSS_u^2 - \frac{V_{i,t}\eta_{i,t}}{G_{i,t}} IFSS_t^2 \right) \quad (2)$$

where the subscripts t and u refer to the surface treated and untreated composites, respectively, and η is the loss factor. The damping versus IFSS plot is represented as a parabola centered on the ordinate axis where the coefficient depends on the volume fraction, the shear modulus, and the loss factor of the specific interphase. This result may sound discordant with the linear plot found by Murayama and Lawton, but these two plots, in fact, represent two physically different mechanisms of damping.

3. Fabrication

3.1. Materials

Unidirectional fibers from Toray Industries, Inc., Japan were used in this work. The main properties are a tensile strength of 4.9 GPa and a longitudinal tensile modulus of 230 GPa with a filament diameter of 7 μm . The epoxy resin and the hardener were purchased from Mike Compositi, Milan, Italy. The two components are given in a pack, called epoxy system SX8 EVO, where the mix ratio is prescribed to be 100:30 (resin to hardener) and the reaction dynamic is classified as medium velocity. The silane coupling agents used are (3-Aminopropyl)triethoxysilane commercial name: APTES and (3-Glycidyloxypropyl)trimethoxysilane, commercial name: GLYMO. Both were produced by Aldrich and supplied by Merck Life Science S.r.l.

3.2. Process

The fiber surface treatment is a two-way treatment since oxidation is performed before the silane coupling treatment. This process, even longer to perform, can guarantee a stronger interphase when compared to the silane coupling treatment alone [14,15].

Air oxidation is performed on the as-received fibers in an oven at 200°C for 2 hours. Then, two different solutions must be prepared for the two different silanes:

- APTES: 5% silane, 90% ethanol, 5% distilled water
- GLYMO: 1% silane, 99% distilled water

To dissolve the silane, both solutions have been hot stirred for 1 hour at 50°C. Once the solution is ready, it is applied to the fibers in a bath at ambient temperature for 1 hour. Fibers are successively dried in the oven at 100°C for 3 hours. The final composites are realized with a liquid resin infusion (LRI) technique under vacuum and then cured overnight in an oven.

3.3. Thicknesses analysis

The first quantitative effect of the silanes can be noted right after manufacturing. By measuring the plate thickness in different positions, an average thickness and an incertitude value for that measure can be computed for each plate. Results are presented in Table 1, where AR stands for as-received fibers. The maximum relative error is below 5% which is low for an experimental type of fabrication. It can be noted that the plates realized with untreated fibers (AR) are thinner than the ones composed of treated fibers (GLYMO and APTES), and that there is a significant difference of approximately 17% between the average thicknesses of the plates with the two different silanes. While the smaller thickness of the AR plates can be easily explained by acknowledging the fact that there is no additional interphase material, so the interphase, although still present, will forcefully be thinner than the silane-treated plates ones. The origin of the thickness difference between the two

silane-treated plates is less clear. Indeed, APTES plates are thicker than GLYMO plates on average. But, when we look at the molecules that constitutes the respective interphases, the GLYMO has a higher molecular weight and a longer chain too. The explanation of this result may lie on the solution compositions: APTES silane was applied to a 5% concentrated solution, while GLYMO was just a 1% concentrated. Therefore, at equal weights of solution applied, the GLYMO plates will have a lower number of silane molecules than the APTES plates, resulting in an extended interphase. The density data confirm the hypothesis: the as-received plate has a higher density while the APTES plate is less dense than the GLYMO one. This is because the APTES plate contains a higher volume of low-density interphase material. Therefore, when the density of the composite is calculated through the rule of mixture, the volume fraction of the interphase is higher than it is in the GLYMO calculation, and it raises the weight of the low-density interphase term.

Table 1. Thicknesses and densities of the fabricated plates

	Thickness [mm]	Incertitude [mm]	Density [g/cm^3]
AR	1.94	0.06	1.31
GLYMO	2.37	0.09	1.25
APTES	2.96	0.14	1.18

4. Experimental tests

Damping was evaluated through the free decay test on specimens cut from the fabricated plates into beam-shaped specimens in 148 mm of length and 19 mm in width. The experimental setup is represented in Figure 1.

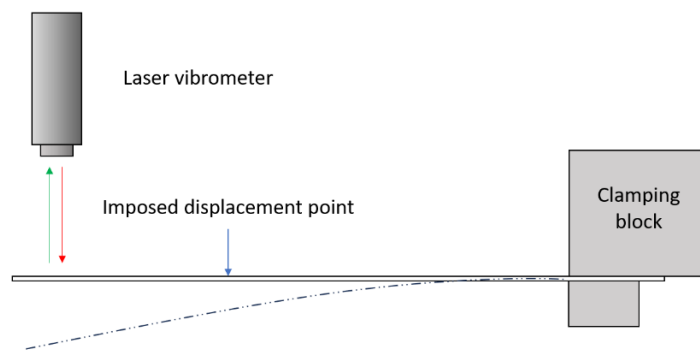


Figure 1. Setup scheme for the free decay test, specimen blocked on one side

A preliminary test campaign was conducted to determine an appropriate initial displacement to utilize for the free decay tests. A free decay test was performed at different initial displacements of the tip. Finally, a standard displacement was set equal for all the specimens.

The final free decay test campaign was conducted on 8 specimens per type of material. Each specimen was tested three times, and an average value was taken, making it statistically relevant. Figures 3 and 4 summarize the results of this experimental test campaign.

The presented results refer to specimens made of 8 layers all oriented at $[0^\circ]_8$, i.e. in the specimen longitudinal direction. As can be noted, especially from the bar plot, the differences in damping between the different materials are more marked on $[0^\circ]_8$ beams. This is because in these materials the interface is more stressed. When a $[90^\circ]_8$ specimen is inflected instead, all the deformation is distributed on the matrix, since there is little to no load transfer between fibers and matrix, the interphase is nearly unloaded and its contribution to damping is minimal.



Figure 2. Setup for the free decay test, specimen blocked on one side

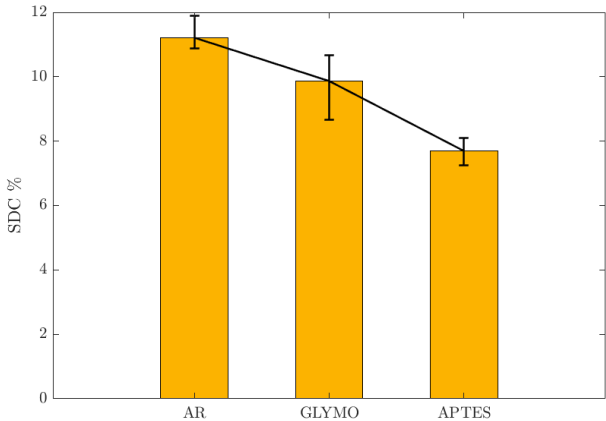


Figure 3. Comparison of free decay damping between the different materials, [0°]₈ specimen

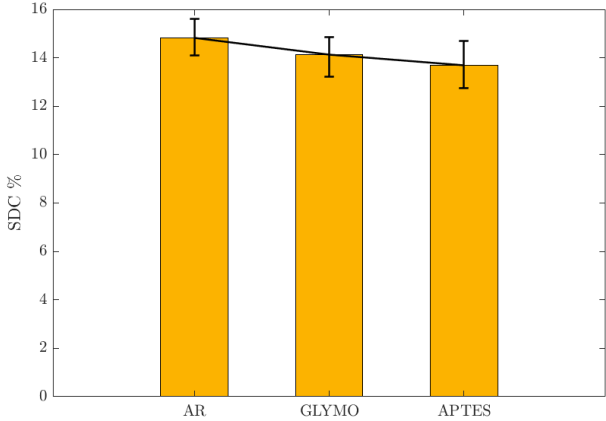


Figure 4. Comparison of free decay damping between the different materials, [90°]₈ specimen

5. Conclusions and perspectives

The study is composed of two phases: a fabrication phase designed from the engineering and chemical points of view to obtain the desired interphases and a testing phase aimed at measuring the properties of the obtained specimens. The investigation yielded some attended results and some new insight. The surface treatment turned out to relevantly affect the final product thickness. This finding can be explained by thinking of the volume of silane that was added to the solution for fiber treatment. Density data confirms the assumption. Although a formula to predict the final product thickness is still not available, these findings demonstrate the necessity of including a term that

accounts for the surface treatment, as a key contributor to the final thickness and weight of the product.

Vibrational tests of these latter specimen have confirmed the acknowledged fact that an improvement in the interphase shear strength causes a decrease in damping of the material. Indeed, lower interphase strength means a higher portion of detached interphase for a fixed level of strain. In turn, this means that more energy is dissipated for a fixed level of strain. As a perspective to the present work, a more extensive modal analysis may be performed to check if the same pattern is present also on modes of higher order, of particular interest are torsion modes.

From a theoretical point of view instead, the relationship between damping and interphase strength has been analyzed. In the present work, a three-phase model has been exploited to analytically predict the relation, and it turned out to be a quadratic relationship instead of a linear one as it was believed to be. This finding, however, is not in complete discordance with the existing plot because they represent two different mechanisms of damping. This relationship though still has to be validated. The interface strength measures are needed to produce a plot of damping versus interface strength. Further studies may also find that it is the stiffness of the interphase that determines damping in an intact state more than the interphase shear strength.

Acknowledgements

The first author wishes to thank the University of Pisa and the Italian Scientists and Scholars in North America Foundation (ISSNAF) for supporting his stay at the Ray W. Herrick Laboratories of the School of Mechanical Engineering at Purdue University.

All authors would like to thank the University of Pisa for funding through the PRA 2022–2023 project titled “Advanced modelling of ultra-lightweight materials and structures”.

6. References

- [1] X. Tang and X. Yan, “A review on the damping properties of fiber reinforced polymer composites”, *J. Ind. Text.*, vol. 49, no. 6, pp. 693–721, 2020.
- [2] J. M. Kennedy, D. D. Edie, A. Banerjee, and R. J. Cano, “Characterization of interfacial bond strength by dynamic analysis”, *J. Compos. Mater.*, vol. 26, no. 6, pp. 869–882, 1992.
- [3] S. H. Aziz and M. P. Ansell, “The effect of alkalization and fibre alignment on the mechanical and thermal properties of kenaf and hemp bast fibre composites: Part 1–polyester resin matrix”, *Compos. Sci. Technol.*, vol. 64, no. 9, pp. 1219–1230, 2004.
- [4] T. Doan, H. Brodowsky, and E. Mäder, “Jute fibre/polypropylene composites II. Thermal, hydrothermal and dynamic mechanical behaviour”, *Compos. Sci. Technol.*, vol. 67, no. 13, pp. 2707–2714, 2007.
- [5] V. G. Geethamma, G. Kalaprasad, G. Groeninckx, and S. Thomas, “Dynamic mechanical behavior of short coir fiber reinforced natural rubber composites”, *Compos. Part A Appl. Sci. Manuf.*, vol. 36, no. 11, pp. 1499–1506, 2005.
- [6] S. K. Chaturvedi and G. Y. Tzeng, “Micromechanical modeling of material damping in discontinuous fiber three-phase polymer composites”, *Compos. Eng.*, vol. 1, no. 1, pp. 49–60, 1991.
- [7] T. Murayama and E. L. Lawton, “Dynamic loss energy measurement of tire cord adhesion to rubber”, *J. Appl. Polym. Sci.*, vol. 17, no. 3, pp. 669–677, 1973.
- [8] B. Z. Jang, “Control of interfacial adhesion in continuous carbon and kevlar fiber reinforced polymer composites”, *Compos. Sci. Technol.*, vol. 44, no. 4, pp. 333–349, 1992.
- [9] A. S. Tikhomirov, N. E. Sorokina, and V. V. Avdeev, “Surface modification of carbon fibers with nitric acid solutions”, *Inorg. Mater.*, vol. 47, pp. 609–613, 2011.

- [10]X. Qian, Y. G. Zhang, X. F. Wang, Y. J. Heng, and J. H. Zhi, "Effect of carbon fiber surface functionality on the moisture absorption behavior of carbon fiber/epoxy resin composites", *Surf. Interface Anal.*, vol. 48, no. 12, pp. 1271–1277, 2016.
- [11]T. Sun, M. Li, S. Zhou, M. Liang, Y. Chen, and H. Zou, "Multiscale structure construction of carbon fiber surface by electrophoretic deposition and electropolymerization to enhance the interfacial strength of epoxy resin composites", *Appl. Surf. Sci.*, vol. 499, no. 143929, 2020.
- [12]D. Xu, B. Liu, G. Zhang, S. Long, X. Wang, and J. Yang, "Effect of air plasma treatment on interfacial shear strength of carbon fiber–reinforced polyphenylene sulfide", *High Perform. Polym.*, vol. 28, no. 4, pp. 411–424, 2016.
- [13]B. Yu, Z. Jiang, X. Tang, C. Y. Yue, and J. Yang, "Enhanced interphase between epoxy matrix and carbon fiber with carbon nanotube-modified silane coating", *Compos. Sci. Technol.*, vol. 99, pp. 131–140, 2014.
- [14]J. Shi, Y. Yamamoto, M. Mizuno, and C. Zhu, "Interfacial performance enhancement of carbon fiber/epoxy composites by a two-step surface treatment", *J. Mech. Sci. Technol.*, vol. 35, pp. 91–97, 2021.
- [15]Z. Wen, C. Xu, X. Qian, Y. Zhang, X. Wang, S. Song, M. Dai, and C. Zhang, "A two-step carbon fiber surface treatment and its effect on the interfacial properties of CF/EP composites: The electrochemical oxidation followed by grafting of silane coupling agent", *Appl. Surf. Sci.*, vol. 486, pp. 546–554, 2019.
- [16]S. H. Wang, L. L. Yao, J. H. Jin, G. Li, and S. L. Yang, "Effect of air oxidation treatment on interfacial properties of carbon fibers", *Mater. Sci. Forum*, vol. 993, pp. 695–700, 2020.
- [17]E. E. Ungar and E. M. Kerwin Jr, "Loss factors of viscoelastic systems in terms of energy concepts", *J. Acoust. Soc. Am.*, vol. 34, no. 7, pp. 954–957, 1962.
- [18]S. N. Durukan, B. Beylergil and C. Dulgerbaki, "Effects of silane-modified nano-CaCO₃ particles on the mechanical properties of carbon fiber/epoxy (CF/EP) composites", *Polymer Composites*, vol. 44, no. 3, pp. 1805-1821, 2023.
- [19]S. Xiong, Y. Zhao, Y. Wang, J. Song, X. Zhao and S. Li, "Enhanced interfacial properties of carbon fiber/epoxy composites by coating carbon nanotubes onto carbon fiber surface by one-step dipping method.", *Applied Surface Science*, vol. 546, pp. 149-135, 2021.